HHS Public Access

Author manuscript

J Membr Biol. Author manuscript; available in PMC 2016 June 01.

Published in final edited form as:

J Membr Biol. 2015 June ; 248(3): 419–430. doi:10.1007/s00232-015-9805-x.

Voltage Sensing in Membranes: From Macroscopic Currents to Molecular Motions

J. Alfredo Freites[1] and **Douglas J. Tobias**[1]

J. Alfredo Freites: jfreites@uci.edu

[1]Department of Chemistry, University of California, Irvine, CA 92697-2025, USA

Abstract

Voltage-sensing domains (VSDs) are integral membrane protein units that sense changes in membrane electric potential, and through the resulting conformational changes, regulate a specific function. VSDs confer voltage-sensitivity to a large superfamily of membrane proteins that includes voltage-gated Na^+, K^+, Ca^{2+}, and H^+ selective channels, hyperpolarization-activated cyclic nucleotide-gated channels, and voltage-sensing phosphatases. VSDs consist of four transmembrane segments (termed S1 through S4). Their most salient structural feature is the highly conserved positions for charged residues in their sequences. S4 exhibits at least three conserved triplet repeats composed of one basic residue (mostly arginine) followed by two hydrophobic residues. These S4 basic side chains participate in a state-dependent internal salt-bridge network with at least four acidic residues in S1–S3. The signature of voltage-dependent activation in electrophysiology experiments is a transient current (termed gating or sensing current) upon a change in applied membrane potential as the basic side chains in S4 move across the membrane electric field. Thus, the unique structural features of the VSD architecture allow for competing requirements: maintaining a series of stable transmembrane conformations, while allowing charge motion, as briefly reviewed here.

Keywords

Voltage-sensing domains; Voltage gating; Gating currents; Voltage-gated channels; Membrane potential; Membrane proteins

Gating Currents and Their Molecular Origin

Excitable cells use changes in the membrane potential to relay information, in the form of electrical signals, resulting in cell activity. The notion that function regulated by the membrane potential requires a voltage-sensing mechanism embedded in the membrane was first introduced by Hodgkin and Huxley to describe the regulation of ion permeation by an applied membrane potential in the squid giant axon (Hodgkin and Huxley 1952). The physical basis of cell excitability, as postulated by Hodgkin and Huxley, is the motion of charged particles within the membrane electric field upon a change in membrane potential leading to the opening and closing of ion channels. Direct evidence of the motion of these so-called gating (or sensing) charges was first reported by Armstrong and Bezanilla, Keynes and Rojas, and Schneider and Chandler, who established that macroscopic gating currents appear as a transient nonlinear capacitive component of the membrane current in voltage-

clamped experiments on the squid giant axon (Armstrong and Bezanilla 1973; Bezanilla and Armstrong 1974; Keynes and Rojas 1973) and frog skeletal muscle (Schneider and Chandler 1973). Membrane depolarization was found to elicit an outward gating current, whereas repolarization generates an inward gating current (Fig. 1).

The gating charge magnitude as a function of membrane potential (the so-called *Q*–*V* curve, see Fig. 1b) is usually described by the corresponding ensemble average using a Boltzmann distribution over two states, denoted resting and activated, or including a small number of intermediate states. In the simple two-state case it is expressed as (Hille 2001)

$$Q(V)=\frac{Q_0}{1+e^{-z(V-V_{1/2})/k_BT}}, \quad (1)$$

where Q_0 is the maximum gating charge, $V_{1/2}$ is the mid-point potential, and z is a charge equivalent.

The measured charge displacement is given by

$$Q=\sum_i q_i\delta_i, \quad (2)$$

where q_i represent the magnitude of the actual atomic charges, δ_i is the corresponding fraction of the membrane electric field they traverse, and the sum is over all the charged atoms involved in the gating transition.

The first sequencing and cloning of a voltage-dependent membrane protein was the voltage-gated Na^+ (Na_V) channel from *Electrophorus electricus* (Noda et al. 1984). Sequencing of the voltage-gated Ca^{2+} (Ca_V) channel from skeletal muscle (Tanabe et al. 1987) and the K^+ (K_V) channel encoded by the *Shaker* gene of *Drosophila* (Tempel et al. 1987) strengthen the notion that voltage-gated ion channels form a protein superfamily with a common activation mechanism (Hille 2001). When knowledge of the first channel sequence (Noda et al. 1984) was combined with the evidence from gating current studies (Armstrong 1981), the first molecular models of voltage-dependent activation quickly followed (Noda et al. 1984; Kosower 1985; Greenblatt et al. 1985; Guy and Seetharamulu 1986; Catterall 1986). Voltage-gated cation channels were found to consist of four homologous domains (as either tandem regions of a single protein chain in Na_V and Ca_V channels or as four separate protein chains in K_V channels), each comprising six transmembrane helical segments, termed S1 through S6 by Noda et al. (1984) (Fig. 2a). The S4 segment, which is rich in basic side chains and exhibits a conserved sequence triplet motif consisting of one basic residue (mostly arginine) followed by two hydrophobic residues (Fig. 3) was proposed as the voltage-sensing element in voltage-gated cation channels (Noda et al. 1984; Tempel et al. 1987; Greenblatt et al. 1985; Guy and Seetharamulu 1986; Catterall 1986). Charge pairing between the basic residues in S4 and acidic residues in the surrounding transmembrane segments was also invoked as a way to stabilize S4 within the membrane dielectric (Armstrong 1981; Greenblatt et al. 1985; Guy and Seetharamulu 1986; Catterall 1986).

Cloning of voltage-dependent cation channels introduced the ability to study a specific channel in virtual isolation, by expressing it in oocytes or mammalian cell lines with low background of intrinsic membrane currents. Expression in these systems can achieve substantially higher channel densities than in natural tissues such as the squid giant axon, and advances in instrumentation allow measurements of electrical currents from a controlled number of channels at large signal-to-noise ratios (Sakmann and Neher 1984). The combination of these techniques with site-directed mutagenesis started the era of structure–function relationship studies in voltage-gated ion channels. It was shown early on that not only the charged residues themselves but also the specificity of the triplet motif in the S4 segment play a key role in voltage-dependent activation (Stühmer et al. 1989; Auld et al. 1990; Papazian et al. 1991; Liman et al. 1991; McCormack et al. 1991). Neutralization of S4 charges was found to alter the magnitude of the total gating charge (Schoppa et al. 1992; Aggarwal and MacKinnon 1996; Seoh et al. 1996). Similarly, site-directed mutagenesis also proved a role in voltage-dependent activation for charge pairing between S4 and the S2 and S3 segments (Papazian et al. 1995; Planells-Cases et al. 1995; Seoh et al. 1996; Tiwari-Woodruff et al. 2000).

Early gating current experiments used signal subtraction techniques to identify the gating current (Armstrong 1981). The era of optimized expression systems brought the first direct measurement of isolated gating currents in mammalian brain Na_V channel (Conti and Stühmer 1989), *Shaker* K_V channel (Bezanilla et al. 1991), and mammalian cardiac Ca_V channel (Neely et al. 1993). The discrete nature of the gating current, central to the Hodgkin and Huxley hypothesis, was verified by fluctuation analyses of gating current recordings, which revealed the magnitude of the elementary charge movements to be on the order of 2 *e* (Conti and Stühmer 1989; Crouzy and Sigworth 1993; Sigg et al. 1994). Sigg et al. (1994) performed their measurements on a variant of the *Shaker* channel in which all traces of ionic current were inherently abolished (Perozo et al. 1993), which allowed them to follow the time course of the gating current with enough detail to perform kinetic modeling. Their analysis showed that the elementary contributions to the gating current occur at two different time scales, with the main fluctuation of 2.4 *e* preceded by smaller and faster contributions.

Voltage-Sensing Domains as Modular Functional Units

In the tradition of Hodgkin and Huxley (1952), electrophysiology experiments are modeled using kinetic theory. Constraints from detailed analyses of gating currents and the control of the ionic currents via molecular manipulations have produced a series of sophisticated kinetic models of voltage-dependent activation (Zagotta et al. 1994; Schoppa and Sigworth 1998; Ledwell and Aldrich 1999), which assume that each S4 segment moves independently between the channel resting state and a pre-open activated state, followed by a concerted transition that opens the pore domain gate. Thus, at the core of these models is the idea that voltage-gated channels are modular entities.

The notion of separate domains for selective permeation and voltage-dependent activation in voltage-gated channels originates in the first reports on the identification and functional characterization of non-voltage-dependent K^+ channels spanning only two transmembrane segments per subunit and exhibiting a high degree of homology to the S5 through S6

conserved regions of K_V channels; the list includes two inward-rectifying mammalian channels (Kubo et al. 1993; Ho et al. 1993), and the prokaryotic K^+ channel from *Streptomyces lividans* (KcsA) (Schrempf et al. 1995), which only a few years later yielded the first atomic resolution ion channel structure (Doyle et al. 1998). Perhaps the first clear evidence for the existence of a voltage-sensing domain (VSD) as an evolutionary conserved functional module in voltage-gated channels came from the studies by Li-Smerin and Swartz of binding specificity of tarantula venom peptide toxins. Two different but highly homologous toxins known to target specific K_V and Ca_V channels by modifying their voltage-dependent activation were shown to bind to a similar region in both K_V or Ca_V channels between the S3 and S4 segments (Li-Smerin and Swartz 1998). Functional modularity in voltage-gated channels was finally proven by Lu and coworkers, who showed that VSDs from the *Shaker* K_V channel engineered into the non-voltage-gated KcsA confer strong voltage dependence (Lu et al. 2002, 2001).

The next breakthrough in the study of voltage sensing across membranes is the atomic resolution crystallographic structures of prokaryotic and eukaryotic K_V channels reported by MacKinnon and collaborators (Jiang et al. 2003a; Lee et al. 2005; Long et al. 2005, 2007; Chen et al. 2010), as well as the most recent structures of bacterial Na_V channels (Payandeh et al. 2012; Zhang et al. 2012). These structures reveal a conserved modular architecture for voltage-gated ion channels from Archaea to mammals, in which VSDs comprised by the S1 through S4 segments appear as independent structural units loosely attached to a central pore domain (Fig. 2b). Further reinforcing the idea of the S1–S4 VSD as a modular unit, the isolated VSD from the thermophile *Aeropyrum pernix* K_V channel (KvAP) has been expressed in bacteria, crystallized (Jiang et al. 2003a), and reconstituted into micellar and membrane environments (Chakrapani et al. 2008; Krepkiy et al. 2009; Butterwick and MacKinnon 2010; Gupta et al. 2011).

Another striking development during the last ten years was the discovery of two new membrane protein families containing VSDs but lacking separate pore domains. The voltage-gated proton channel (Hv1) (Ramsey et al. 2006; Sasaki et al. 2006) is a pH-sensitive proton-selective voltage-dependent channel with a homodimeric functional unit (Koch et al. 2008; Lee et al. 2008; Tombola et al. 2008). Each subunit forms a VSD with a gated proton permeation pathway, which is presumably shared with the translocation pathway of the S4 charges during gating (Koch et al. 2008; Tombola et al. 2008). The voltage-sensing phosphatase (VSP) (Murata et al. 2005) is a family of enzymes consisting of a single VSD and a cytoplasmic domain of phosphoinositide phosphatase homologous to phosphatase and tensin homolog (PTEN) (Kohout et al. 2008). Similar to voltage-gated cation channels, the VSD in VSP has been shown to regulate the catalytic domain through an electromechanical coupling mechanism that depends on the specificity of the linker between the two domains (Murata and Okamura 2007; Kohout et al. 2010).

The crystallographic and solution NMR structures from voltage-gated cation channels show the VSD in a similar “up” conformation with S4 closer to the extracellular side of the membrane. In contrast, the VSD crystallographic structures for VSP from *Ciona intestinalis* (Ci-VSP) and Hv1 from mouse, reported recently (Li et al. 2014; Takeshita et al. 2014), show the VSD in a “down” conformation with S4 closer to the intracellular side. Given that

the *Q–V* curves of Hv1 and VSP are shifted to more positive potentials than K_V and Na_V channels, these results suggest that the “up” and “down” conformations observed in the VSD structures determined in the absence of a membrane potential may reflect, respectively, structures close to and away from the VSD activated state. Following this reasoning, to stabilize the up state in the absence of a membrane potential, Li et al. (2014) also determined the structure of the R217E Ci-VSP variant whose *Q–V* curve is negatively shifted with respect to wild-type. Comparison of the two structures largely confirms the mechanistic features inferred from functional studies on voltage-gated cation channels.

Voltage-Sensing Domain Solvation in the Membrane

The available structures show the VSD as a four-helix bundle shaped like an hourglass, with two crevices open to the extracellular and intracellular aqueous media, and a central constriction (Fig. 4a) (Jiang et al. 2003a; Long et al. 2007; Chen et al. 2010; Butterwick and MacKinnon 2010; Payandeh et al. 2012; Zhang et al. 2012; Li et al. 2014; Takeshita et al. 2014). In most structures, the crevices are separated by a cluster of hydrophobic residues, featuring a highly conserved Phe in S2 and Ile in S1 (Palovcak et al. 2014) (Fig. 3). All four transmembrane segments have a face exposed to the lipid bilayer hydrocarbon core, but the conserved S4 basic side chains and S1–S3 acidic side chains (Palovcak et al. 2014) are either housed in the crevices, where they are engaged in salt-bridge interactions, or are placed at locations where they would be exposed to the membrane–water interface (Fig. 4a). Molecular models of membranes embedded with VSDs from atomistic molecular dynamics (MD) simulations predicted that the lipid bilayer would arrange itself around the VSD so as to maximize the interactions of the headgroups with the ends of the VSD, which are decorated with polar, aromatic, and charged residues (Fig. 4b) (Freites et al. 2006; Sands and Sansom 2007; Treptow and Tarek 2006; Jogini and Roux 2007). This rearrangement of the membrane interface allows waters to penetrate deeply into the hourglass architecture where they solvate the internal salt-bridge network. All of the S4 charges exhibit a complete solvation shell consisting of waters, carboxyl groups or anionic lipid head groups, with the exact composition of each solvation shell depending on the conformation of the VSD, and the position of the basic side chain in the S4 segment (Treptow and Tarek 2006; Krepkiy et al. 2009; Schow et al. 2010).

The predictions from atomistic simulations were later confirmed by a series of structural studies on the isolated KvAP VSD embedded in membrane model systems. Site-directed spin labeling and EPR spectroscopy revealed water filled crevices that are consistent with the hydration patterns observed in the atomistic MD simulations (Chakrapani et al. 2008). Transmembrane density profiles from lamellar neutron diffraction experiments showed distortions in the lipid bilayer and water penetration that were consistent with simulation systems prepared to mimic the density and composition of the experimental systems (Krepkiy et al. 2009). Solid-state NMR data showed short-range interactions between the S4 charges and the same set of solvation partners predicted by atomistic simulations (Krepkiy et al. 2009, 2012). Finally, a H–D exchange transmembrane profile determined by neutron interferometry from solid-supported VSDs monolayers solubilized in detergent, in which the VSD exhibit a similar transmembrane profile as the VSD structure from solution NMR

(Butterwick and MacKinnon 2010), was found to reproduce the transmembrane profile from simulations of the VSD embedded in a lipid bilayer (Gupta et al. 2012).

Full internal hydration of the VSD embedded in a membrane is consistent with a large body of evidence from Cys scanning mutagenesis combined with accessibility assays employing small thiol-reactive compounds, which revealed that the S4 charges were exposed to the extracellular and intracellular aqueous media, and that the pattern of exposure (i.e., which specific sidechains were exposed to the intracellular or extracellular side) was voltage-dependent (Larsson et al. 1996; Baker et al. 1998; Yang and Horn 1995; Yang et al. 1996, 1997; Yusaf et al. 1996; Wang et al. 1999). Complementary site-directed fluorescence measurements strongly suggested that changes in S4 accessibility are due to VSD conformational changes that occur during voltage-dependent activation (Mannuzzu et al. 1996; Cha and Bezanilla 1997; Gandhi et al. 2003; Pathak et al. 2007).

Non-conducting VSDs from K_V and Na_V channels may be rendered permeable to cations or protons by mutation of the S4 charges (Starace et al. 1997; Starace and Bezanilla 2001, 2004; Tombola et al. 2005, 2007; Sokolov et al. 2005, 2007, 2010). This finding strongly suggests that the motion of charges within the VSD occurs through a hydrophilic permeation pathway that is blocked in native VSDs of voltage-gated cation channels and VSPs (Tombola et al. 2007; Campos et al. 2007).

Taken together, results from both structural and functional studies converge to the principle that the architecture of the VSD is optimized to allow for stable voltage-dependent transmembrane conformations that result in net charge displacements within the membrane electric field. Indeed, the experimental evidence strongly suggests that the electric field is not uniform in membranes embedded with VSDs. Instead, the membrane dielectric barrier is expected to be substantially shorter within the VSD than the 30–40 Å thickness of the lipid bilayer hydrocarbon core, a phenomenon referred in the literature as “focusing” of the membrane electric field (Fig. 5c) (Islas and Sigworth 2001; Ahern and Horn 2005; Starace and Bezanilla 2004).

The discovery of the two additional protein families described above gives rise to the notion of a superfamily of protein containing S1–S4 VSDs. A recent study (Palovcak et al. 2014) reported a statistical analysis of a large multiple sequence alignment of VSD sequences encompassing the whole superfamily. In addition to the expected conservation of functionally relevant residues, Palovcak et al. (2014) found evolutionarily constrained networks that define the interfaces between S1–S2 and S2–S3 but not with S4. The solvation of the VSD, as described here, is reflected in the nature of the coevolving residue contacts that line the interior of the VSD. In addition, coevolving residue pairs were identified that would only have occurred in the resting conformation of the VSD. Thus, the core structure–function relationships of VSDs described so far can be recast as evolutionary design principles.

Motion of Gating Charges in Voltage-Sensing Domains

It is now well established that voltage-dependent conformational changes in VSDs involve the displacement of the S4 segment. The available experimental evidence and molecular

models also suggest that sequential charge pair formation between the basic side chains in S4 and the conserved acidic sidechains in S1–S3 is a structural signature of voltage-sensing motion (Papazian et al. 1995; Tiwari-Woodruff et al. 1997; DeCaen et al. 2008, 2009, 2011; Delemotte et al. 2011; Henrion et al. 2012). The formation of these salt-bridges has been shown to be strictly necessary for the partitioning and assembly of VSDs in the ER membrane and for their surface expression (Papazian et al. 1995; Tiwari-Woodruff et al. 1997; Zhang et al. 2007), but the Coulomb interactions that could help stabilize the transmembrane topology during protein maturation are likely to be weakened in the hydrated interior of the VSD. Thus, the role of sequential charge pair formation during voltage sensing appears to be more subtle than the originally proposed gating charge stabilization (Guy and Seetharamulu 1986; Catterall 1986).

Functional characterization of voltage-gated channel variants where the VSD conserved sites for acidic and basic side chains are neutralized is a classical experiment used to understand the role of charge pair interactions in voltage gating (Papazian et al. 1995) as well as to study the contribution of specific residues to the total gating charge the VSD (Seoh et al. 1996). Ahern and coworkers (Pless et al. 2011) recently revisited the case of contributions to the voltage-sensing function of two of the conserved acidic side chains in the S2 and S3 segments in the *Shaker* channel (E293 and D316, respectively). Previous studies achieved charge neutralization by mutating each acidic residue to the corresponding amide (i.e Glu to Gln and Asp to Asn), and reported that electrostatic interactions between S4 arginines and these two residues were key to the voltage-sensing function (Papazian et al. 1995; Seoh et al. 1996) in *Shaker*. Pless et al. (2011) argued that such substitution does not abolish the electrostatic interaction but instead introduces a potential hydrogen bond donor group in place of the acidic side chain. They compared the behavior of the amidated side chain to the mutation to the unnatural amino acid nitrohomoalanine, whose nitro functional group is isosteric and isoelectronic to the carboxyl group. Remarkably, while the amidated substitutions altered the voltage dependence of the channel conductance, the neutralization produced no effect on either site. The same experiment performed on the third conserved side-chain (E283 in S2), which is considered to be central to the stabilization of the activated state of the VSD due to the inferred electrostatic interactions with two inner Args of S4, produced only a mild shift in the stability of the channel open state to more positive voltages, but a completely new phenotype upon amidation. They concluded that the main role of charge pairing in the interior of the VSD is not stabilization of a transmembrane conformation through Coulomb interactions. Rather, they suggested, given the abundant evidence reviewed in the previous section, that these charge pairings facilitate the internal hydration of the VSD, thereby contributing to a more polar environment for the motion of the S4 charges.

Recent atomistic MD simulations on the 10-μs timescale of the KvAP VSD in a hydrated lipid bilayer (Freites et al. 2012) provide a model for the generation of gating charge displacements consistent with the results of Pless et al. (2011). These simulations recorded a net gating charge displacement of 1 *e* upon membrane repolarization, which was produced by the concerted motion of three S4 basic side chains. The S4 charges remained fully hydrated at all times and their motion was characterized as water-catalyzed charge pair

exchanges with the conserved acidic side chains in S1–S3 (Fig. 6) (Freites et al. 2012). Similar observations were made in 100-μs timescale atomistic simulations of a full-length eukaryotic K_V channel by Jensen et al. (2012).

The evidence discussed so far establishes the internal hydration of the VSD as a key element of the voltage-sensing mechanism but it does not answer the question of how the S4 segment remains stable as a transmembrane helix during voltage-dependent activation. All the available VSD structures in the "up" conformation show the S4 segment forming a helix-turn-helix motif with the C-terminal half of S3, termed the voltage-sensing paddle by MacKinnon and coworkers (Jiang et al. 2003a), who suggested could be considered as a hydrophobic cation (Jiang et al. 2003b). Subsequently, Swartz et al. (Alabi et al. 2007; Bosmans et al. 2008) demonstrated that the voltage-sensing paddle was a modular, portable unit by engineering fully functional eukaryotic K_V chimeric channels containing paddle motifs from KvAP, Ci-VSP, Hv1 and Na_V VSDs. Consistent with the analyses of Palovcak et al. (2014), discussed in the previous section, the results by Swartz and coworkers suggest that there are no evolutionary constraints between the voltage-sensing paddle motif and the rest of the VSD. Furthermore, an extensive analysis of the interaction of these chimeras with tarantula venom toxins places the paddle motif in the lipid membrane environment (Alabi et al. 2007). More recently, Lu et al. used state-dependent engineered disulfide bond formation to show that the voltage-sensing paddle exists in functional *Shaker* channels expressed in oocytes (Xu et al. 2013). In that same study, Lu and coworkers report an extensive electrophysiological study on deletion mutants showing that hydrophobic interactions between S3 and S4 in the voltage-sensing paddle are the key to the stabilization of the channel in the open state (Xu et al. 2013). Thus, the functional role of the voltage-sensing paddle is suggested to be the energetic stabilization of the S4 segment in a helical conformation during voltage-dependent activation.

Voltage-Dependent Structural Studies

A complete mechanistic model of voltage sensing in membranes will require the full characterization of voltage-dependent conformational changes in VSDs with atomic resolution. It is apparent that the inherent limitation of conventional structural determination techniques to probe membrane-embedded protein samples in the presence of a membrane electric field renders them unlikely to achieve this goal. However, the methodological principles of atomic resolution structure determination of macromolecules should remain the same regardless of the specific techniques employed. A macromolecular structure is the end result of a constrained optimization of a molecular model on an empirical potential energy surface. All that is needed is the right combination of experimental observables that can be translated into spatial restraints and used as input to simulations that closely resemble the experimental system.

Alternative conformations of K_V, Na_V and Hv1 VSDs have been generated using atomistic MD simulations of membrane systems combined with experimentally derived distance restraints (Delemotte et al. 2011; Vargas et al. 2011; Henrion et al. 2012; Yarov-Yarovoy et al. 2012) or the combination of positional and distance restraints (Schow et al. 2010). The distance restraints employed were from direct assays or inferred from functional studies.

Despite differences in systems, experimental techniques used to derived restraints, as well as simulation methodologies, all of the models of the VSD in a resting state generated in this manner converge to a similar conformation (Vargas et al. 2012; Souza et al. 2014). A survey of all of these models was recently performed (Souza et al. 2014) to theoretically address a question that cannot be answered through gating current measurement: do gating currents arise exclusively from the motion of charges in a largely immutable membrane electric field or is there a contribution from reshaping of the field accompanying the motion of S4. The findings of Souza et al. (2014) suggest that there are no dynamic changes to the membrane electric field during voltage sensing, implying that functional diversity is a direct reflection of the diversity in the superfamily of proteins containing VSDs.

Voltage-dependent changes in the 1-D transmembrane structure of the VSD from KvAP, vectorially oriented within a phospholipid bilayer membrane, have been recently characterized using time-resolved X-ray and neutron interferometry (Tronin et al. 2014). The results were found to be in good agreement with 1-D distributions from simulations of the KvAP VSD in lipid bilayers in up and down state conformations (Freites et al. 2006; Krepkiy et al. 2009; Schow et al. 2010). This approach could be use to map the voltage-dependent position of specific residues along the transmembrane direction using selective labeling. The combination of this kind of data with state-dependent cross-linking assays (Henrion et al. 2012; Yarov-Yarovoy et al. 2012) could provide a broad-based set of spatial restraints that would be sufficient to refine atomistic models of VSDs using atomistic MD simulations.

Acknowledgments

This work was supported by the National Institutes of Health Grant GM86685. Anton computer time was provided by the National Center for Multiscale Modeling of Biological Systems (MMBioS) through Grant P41GM103712-S1 from the National Institutes of Health and the Pittsburgh Supercomputing Center (PSC). This work used the Extreme Science and Engineering Discovery Environment (XSEDE), which is supported by National Science Foundation Grant number ACI-1053575.

References

Aggarwal SK, MacKinnon R. Contribution of the S4 segment to gating charge in the shaker k+ channel. Neuron. 1996; 16(6):1169–1177. [PubMed: 8663993]

Ahern CA, Horn R. Focused electric field across the voltage sensor of potassium channels. Neuron. 2005; 48(1):25–29.10.1016/j.neuron.2005.08.020 [PubMed: 16202706]

Alabi AA, Bahamonde MI, Jung HJ, Kim JI, Swartz KJ. Portability of paddle motif function and pharmacology in voltage sensors. Nature. 2007; 450(7168):370–375.10.1038/nature06266 [PubMed: 18004375]

Armstrong CM. Sodium channels and gating currents. Physiol Rev. 1981; 61(3):644–683. [PubMed: 6265962]

Armstrong CM, Bezanilla F. Currents related to movement of the gating particles of the sodium channels. Nature. 1973; 242(5398):459–461. [PubMed: 4700900]

Auld VJ, Goldin AL, Krafte DS, Catterall WA, Lester HA, Davidson N, Dunn RJ. A neutral amino acid change in segment iis4 dramatically alters the gating properties of the voltage-dependent sodium channel. Proc Natl Acad Sci USA. 1990; 87(1):323–327. [PubMed: 1688658]

Baker OS, Larsson HP, Mannuzzu LM, Isacoff EY. Three transmembrane conformations and sequence-dependent displacement of the S4 domain in shaker k+ channel gating. Neuron. 1998; 20(6):1283–1294. [PubMed: 9655514]

Bezanilla F, Armstrong CM. Gating currents of the sodium channels: three ways to block them. Science. 1974; 183(4126):753–754. [PubMed: 4821243]

Bezanilla F, Perozo E, Papazian DM, Stefani E. Molecular basis of gating charge immobilization in Shaker potassium channels. Science. 1991; 254(5032):679–683. [PubMed: 1948047]

Bosmans F, Martin-Eauclaire MF, Swartz KJ. Deconstructing voltage sensor function and pharmacology in sodium channels. Nature. 2008; 456(7219):202–208.10.1038/nature07473 [PubMed: 19005548]

Butterwick JA, MacKinnon R. Solution structure and phospholipid interactions of the isolated voltage-sensor domain from KvAP. J Mol Biol. 2010; 403(4):591–606.10.1016/j.jmb.2010.09.012 [PubMed: 20851706]

Campos FV, Chanda B, Roux B, Bezanilla F. Two atomic constraints unambiguously position the s4 segment relative to s1 and s2 segments in the closed state of Shaker K channel. Proc Natl Acad Sci USA. 2007; 104(19):7904–7909.10.1073/pnas.0702638104 [PubMed: 17470814]

Catterall WA. Voltage-dependent gating of sodium channels: correlating structure and function. Trends Neurosci. 1986; 9:7–10.

Cha A, Bezanilla F. Characterizing voltage-dependent conformational changes in the shaker K^+ channel with fluorescence. Neuron. 1997; 19(5):1127–1140. [PubMed: 9390525]

Chakrapani S, Cuello LG, Cortes DM, Perozo E. Structural dynamics of an isolated voltage-sensor domain in a lipid bilayer. Structure. 2008; 16(3):398–409.10.1016/j.str.2007.12.015 [PubMed: 18334215]

Chen X, Wang Q, Ni F, Ma J. Structure of the full-length shaker potassium channel Kv1.2 by normal-mode-based X-ray crystallographic refinement. Proc Natl Acad Sci USA. 2010; 107(25):11352–11357.10.1073/pnas.1000142107 [PubMed: 20534430]

Conti F, Stühmer W. Quantal charge redistributions accompanying the structural transitions of sodium channels. Eur Biophys J. 1989; 17(2):53–59. [PubMed: 2548829]

Crouzy SC, Sigworth FJ. Fluctuations in ion channel gating currents. analysis of nonstationary shot noise. Biophys J. 1993; 64(1):68–76.10.1016/S0006-3495(93)81341-9 [PubMed: 8381683]

DeCaen PG, Yarov-Yarovoy V, Zhao Y, Scheuer T, Catterall WA. Disulfide locking a sodium channel voltage sensor reveals ion pair formation during activation. Proc Natl Acad Sci USA. 2008; 105(39):15142–15147.10.1073/pnas.0806486105 [PubMed: 18809926]

DeCaen PG, Yarov-Yarovoy EM, Scheuer T, Catterall WA. Sequential formation of ion pairs during activation of a sodium channel voltage sensor. Proc Natl Acad Sci USA. 2009; 106(52):22498–22503.10.1073/pnas.0912307106 [PubMed: 20007787]

DeCaen PG, Yarov-Yarovoy V, Scheuer T, Catterall WA. Gating charge interactions with the S1 segment during activation of a Na^+ channel voltage sensor. Proc Natl Acad Sci USA. 2011; 108(46):18825–28830.10.1073/pnas.1116449108 [PubMed: 22042870]

Delemotte L, Tarek M, Klein ML, Amaral C, Treptow W. Intermediate states of the Kv1.2 voltage sensor from atomistic molecular dynamics simulations. Proc Natl Acad Sci USA. 2011; 108(15):6109–6114.10.1073/pnas.1102724108 [PubMed: 21444776]

Doyle DA, Morais Cabral J, Pfuetzner RA, Kuo A, Gulbis JM, Cohen SL, Chait BT, MacKinnon R. The structure of the potassium channel: molecular basis of K^+ conduction and selectivity. Science. 1998; 280(5360):69–77. [PubMed: 9525859]

Freites JA, Tobias DJ, White SH. A voltage-sensor water pore. Biophys J. 2006; 91(11):L90–L92.10.1529/biophysj.106.096065 [PubMed: 17012321]

Freites JA, Schow EV, White SH, Tobias DJ. Microscopic origin of gating current fluctuations in a potassium channel voltage sensor. Biophys J. 2012; 102(11):L44–L46.10.1016/j.bpj.2012.04.021 [PubMed: 22713585]

Gandhi CS, Clark E, Loots E, Pralle A, Isacoff EY. The orientation and molecular movement of a K(+) channel voltage-sensing domain. Neuron. 2003; 40(3):515–525. [PubMed: 14642276]

Greenblatt RE, Blatt Y, Montal M. The structure of the voltage-sensitive sodium channel. Inferences derived from computer-aided analysis of the electrophorus electricus channel primary structure. FEBS Lett. 1985; 193(2):125–134. [PubMed: 2415395]

Gupta S, Liu J, Strzalka J, Blasie JK. Profile structures of the voltage-sensor domain and the voltage-gated K(+)-channel vectorially oriented in a single phospholipid bilayer membrane at the solid-

vapor and solid-liquid interfaces determined by X-ray interferometry. Phys Rev E Stat Nonlin Soft Matter Phys. 2011; 84(3 Pt 1):031911. [PubMed: 22060407]

Gupta S, Dura JA, Freites JA, Tobias DJ, Blasie JK. Structural characterization of the voltage-sensor domain and voltage-gated K+-channel proteins vectorially oriented within a single bilayer membrane at the solid/vapor and solid/liquid interfaces via neutron interferometry. Langmuir. 2012; 28(28):10504–10520. [PubMed: 22686684]

Guy HR, Seetharamulu P. Molecular model of the action potential sodium channel. Proc Natl Acad Sci USA. 1986; 83(2):508–512. [PubMed: 2417247]

Henrion U, Renhorn J, Börjesson SI, Nelson EM, Schwaiger CS, Bjelkmar P, Wallner B, Lindahl E, Elinder F. Tracking a complete voltage-sensor cycle with metal-ion bridges. Proc Natl Acad Sci USA. 2012; 109(22):8552–8557.10.1073/pnas.1116938109 [PubMed: 22538811]

Hille, B. Ion channels of excitable membranes. 3. Sinauer; Sunderland: 2001.

Ho K, Nichols CG, Lederer WJ, Lytton J, Vassilev PM, Kanazirska MV, Hebert SC. Cloning and expression of an inwardly rectifying atp-regulated potassium channel. Nature. 1993; 362(6415): 31–38.10.1038/362031a0 [PubMed: 7680431]

Hodgkin AL, Huxley AF. A quantitative description of membrane current and its application to conduction and excitation in nerve. J Physiol. 1952; 117(4):500–544. [PubMed: 12991237]

Islas LD, Sigworth FJ. Electrostatics and the gating pore of Shaker potassium channels. J Gen Physiol. 2001; 117(1):69–89. [PubMed: 11134232]

Jensen MØ, Jogini V, Borhani DW, Leffler AE, Dror RO, Shaw DE. Mechanism of voltage gating in potassium channels. Science. 2012; 336(6078):229–233.10.1126/science.1216533 [PubMed: 22499946]

Jiang Y, Lee A, Chen J, Ruta V, Cadene M, Chait BT, MacKinnon R. X-ray structure of a voltage-dependent K+ channel. Nature. 2003a; 423(6935):33–41.10.1038/nature01580 [PubMed: 12721618]

Jiang Y, Ruta V, Chen J, Lee A, MacKinnon R. he principle of gating charge movement in a voltage-dependent K+ channel. Nature. 2003b; 423(6935):48.10.1038/nature01581

Jogini V, Roux B. Dynamics of the kv1.2 voltage-gated K+ channel in a membrane environment. Biophys J. 2007; 93(9):3070–3082.10.1529/biophysj.107.112540 [PubMed: 17704179]

Keynes RD, Rojas E. Characteristics of the sodium gating current in the squid giant axon. J Physiol. 1973; 233(1):28P–30P.

Koch HP, Kurokawa T, Okochi Y, Sasaki M, Okamura Y, Larsson HP. Multimeric nature of voltage-gated proton channels. Proc Natl Acad Sci USA. 2008; 105(26):9111–9116.10.1073/pnas.0801553105 [PubMed: 18583477]

Kohout SC, Ulbrich MH, Bell SC, Isacoff EY. Subunit organization and functional transitions in Ci-VSP. Nat Struct Mol Biol. 2008; 15(1):106–108.10.1038/nsmb1320 [PubMed: 18084307]

Kohout SC, Bell SC, Liu L, Xu Q, Minor DL Jr, Isacoff EY. Electrochemical coupling in the voltage-dependent phosphatase Ci-VSP. Nat Chem Biol. 2010; 6(5):369–375.10.1038/nchembio.349 [PubMed: 20364128]

Kosower EM. A structural and dynamic molecular model for the sodium channel of electrophorus electricus. FEBS Lett. 1985; 182(2):234–242. [PubMed: 2579847]

Krepkiy D, Mihailescu M, Freites JA, Schow EV, Worcester DL, Gawrisch K, Tobias DJ, White SH, Swartz KJ. Structure and hydration of membranes embedded with voltage-sensing domains. Nature. 2009; 462(7272):473–479.10.1038/nature08542 [PubMed: 19940918]

Krepkiy D, Gawrisch K, Swartz KJ. Structural interactions between lipids, water and S1–S4 voltage-sensing domains. J Mol Biol. 2012; 423(4):632–647.10.1016/j.jmb.2012.07.015 [PubMed: 22858867]

Kubo Y, Baldwin TJ, Jan YN, Jan LY. Primary structure and functional expression of a mouse inward rectifier potassium channel. Nature. 1993; 362(6416):127–133.10.1038/362127a0 [PubMed: 7680768]

Larsson HP, Baker OS, Dhillon DS, Isacoff EY. Transmembrane movement of the Shaker K^+ channel S4. Neuron. 1996; 16(2):387–397. [PubMed: 8789953]

Ledwell JL, Aldrich RW. Mutations in the s4 region isolate the final voltage-dependent cooperative step in potassium channel activation. J Gen Physiol. 1999; 113(3):389–414. [PubMed: 10051516]

Lee SY, Lee A, Chen J, MacKinnon R. Structure of the KvAP voltage-dependent K^+ channel and its dependence on the lipid membrane. Proc Natl Acad Sci USA. 2005; 102(43):15441–15446.10.1073/pnas.0507651102 [PubMed: 16223877]

Lee SY, Letts JA, Mackinnon R. Dimeric subunit stoichiometry of the human voltage-dependent proton channel hv1. Proc Natl Acad Sci USA. 2008; 105(22):7692–7695.10.1073/pnas.0803277105 [PubMed: 18509058]

Li Q, Wanderling S, Paduch M, Medovoy D, Singharoy A, McGreevy R, Villalba-Galea CA, Hulse RE, Roux B, Schulten K, Kossiakoff A, Perozo E. Structural mechanism of voltage-dependent gating in an isolated voltage-sensing domain. Nat Struct Mol Biol. 2014; 21(3):244–252.10.1038/nsmb.2768 [PubMed: 24487958]

Li-Smerin Y, Swartz KJ. Gating modifier toxins reveal a conserved structural motif in voltage-gated Ca^{2+} and K^+ channels. Proc Natl Acad Sci USA. 1998; 95(15):8585–8589. [PubMed: 9671721]

Liman ER, Hess P, Weaver F, Koren G. Voltage-sensing residues in the S4 region of a mammalian K^+ channel. Nature. 1991; 353(6346):752–756.10.1038/353752a0 [PubMed: 1944534]

Long SB, Campbell EB, Mackinnon R. Crystal structure of a mammalian voltage-dependent shaker family K^+ channel. Science. 2005; 309(5736):897–903.10.1126/science.1116269 [PubMed: 16002581]

Long SB, Tao X, Campbell EB, MacKinnon R. Atomic structure of a voltage-dependent K^+ channel in a lipid membrane-like environment. Nature. 2007; 450(7168):376–382.10.1038/nature06265 [PubMed: 18004376]

Lu Z, Klem AM, Ramu Y. Ion conduction pore is conserved among potassium channels. Nature. 2001; 413(6858):809–813.10.1038/35101535 [PubMed: 11677598]

Lu Z, Klem AM, Ramu Y. Coupling between voltage sensors and activation gate in voltage-gated K^+ channels. J Gen Physiol. 2002; 120(5):663–676. [PubMed: 12407078]

Mannuzzu LM, Moronne MM, Isacoff EY. Direct physical measure of conformational rearrangement underlying potassium channel gating. Science. 1996; 271(5246):213–216. [PubMed: 8539623]

McCormack K, Tanouye MA, Iverson LE, Lin JW, Ramaswami M, McCormack T, Campanelli JT, Mathew MK, Rudy B. A role for hydrophobic residues in the voltage-dependent gating of shaker K^+ channels. Proc Natl Acad Sci USA. 1991; 88(7):2931–2935. [PubMed: 2011602]

Murata Y, Okamura Y. Depolarization activates the phosphoinositide phosphatase Ci-VSP, as detected in xenopus oocytes coexpressing sensors of PIP2. J Physiol. 2007; 583(Pt 3):875–889.10.1113/jphysiol.2007.134775 [PubMed: 17615106]

Murata Y, Iwasaki H, Sasaki M, Inaba K, Okamura Y. Phosphoinositide phosphatase activity coupled to an intrinsic voltage sensor. Nature. 2005; 435(7046):1239–1243.10.1038/nature03650 [PubMed: 15902207]

Neely A, Wei X, Olcese R, Birnbaumer L, Stefani E. Potentiation by the beta subunit of the ratio of the ionic current to the charge movement in the cardiac calcium channel. Science. 1993; 262(5133):575–578. [PubMed: 8211185]

Noda M, Shimizu S, Tanabe T, Takai T, Kayano T, Ikeda T, Takahashi H, Nakayama H, Kanaoka Y, Minamino N. Primary structure of electrophorus electricus sodium channel deduced from cdna sequence. Nature. 1984; 312(5990):121–127. [PubMed: 6209577]

Palovcak E, Delemotte L, Klein ML, Carnevale V. Evolutionary imprint of activation: the design principles of VSDs. J Gen Physiol. 2014; 143(2):145–156.10.1085/jgp.201311103 [PubMed: 24470486]

Papazian DM, Timpe LC, Jan YN, Jan LY. Alteration of voltage-dependence of shaker potassium channel by mutations in the S4 sequence. Nature. 1991; 349(6307):305–310.10.1038/349305a0 [PubMed: 1846229]

Papazian DM, Shao XM, Seoh SA, Mock AF, Huang Y, Wainstock DH. Electrostatic interactions of S4 voltage sensor in shaker K^+ channel. Neuron. 1995; 14(6):1293–1301. [PubMed: 7605638]

Pathak MM, Yarov-Yarovoy V, Agarwal G, Roux B, Barth P, Kohout S, Tombola F, Isacoff EY. Closing in on the resting state of the shaker K(+) channel. Neuron. 2007; 56(1):124–140.10.1016/j.neuron.2007.09.023 [PubMed: 17920020]

Payandeh J, Gamal El-Din TM, Scheuer T, Zheng N, Catterall WA. Crystal structure of a voltage-gated sodium channel in two potentially inactivated states. Nature. 2012; 486(7401):135–139.10.1038/nature11077 [PubMed: 22678296]

Perozo E, MacKinnon R, Bezanilla F, Stefani E. Gating currents from a nonconducting mutant reveal open-closed conformations in shaker K^+ channels. Neuron. 1993; 11(2):353–358. [PubMed: 8352943]

Planells-Cases R, Ferrer-Montiel AV, Patten CD, Montal M. Mutation of conserved negatively charged residues in the S2 and S3 transmembrane segments of a mammalian K^+ channel selectively modulates channel gating. Proc Natl Acad Sci USA. 1995; 92(20):9422–9446. [PubMed: 7568145]

Pless SA, Galpin JD, Niciforovic AP, Ahern CA. Contributions of counter-charge in a potassium channel voltage-sensor domain. Nat Chem Biol. 2011; 7(9):617–623.10.1038/nchembio.622 [PubMed: 21785425]

Ramsey IS, Moran MM, Chong JA, Clapham DE. A voltage-gated proton-selective channel lacking the pore domain. Nature. 2006; 440(7088):1213–1216.10.1038/nature04700 [PubMed: 16554753]

Sakmann B, Neher E. Patch clamp techniques for studying ionic channels in excitable membranes. Annu Rev Physiol. 1984; 46:455–472.10.1146/annurev.ph.46.030184.002323 [PubMed: 6143532]

Sands ZA, Sansom MSP. How does a voltage sensor interact with a lipid bilayer? simulations of a potassium channel domain. Structure. 2007; 15(2):235–244.10.1016/j.str.2007.01.004 [PubMed: 17292841]

Sasaki M, Takagi M, Okamura Y. A voltage sensor-domain protein is a voltage-gated proton channel. Science. 2006; 312(5773):589–592.10.1126/science.1122352 [PubMed: 16556803]

Schneider MF, Chandler WK. Voltage dependent charge movement of skeletal muscle: a possible step in excitation-contraction coupling. Nature. 1973; 242(5395):244–246. [PubMed: 4540479]

Schoppa NE, Sigworth FJ. Activation of Shaker potassium channels. III. an activation gating model for wild-type and V2 mutant channels. J Gen Physiol. 1998; 111(2):313–342. [PubMed: 9450946]

Schoppa NE, McCormack K, Tanouye MA, Sigworth FJ. The size of gating charge in wild-type and mutant Shaker potassium channels. Science. 1992; 255(5052):1712–1715. [PubMed: 1553560]

Schow EV, Freites JA, Gogna K, White SH, Tobias DJ. Downstate model of the voltage-sensing domain of a potassium channel. Biophys J. 2010; 98(12):2857–2866.10.1016/j.bpj.2010.03.031 [PubMed: 20550898]

Schrempf H, Schmidt O, Kümmerlen R, Hinnah S, Müller D, Betzler M, Steinkamp T, Wagner R. A prokaryotic potassium ion channel with two predicted transmembrane segments from Streptomyces lividans. EMBO J. 1995; 14(21):5170–5178. [PubMed: 7489706]

Seoh SA, Sigg D, Papazian DM, Bezanilla F. Voltage-sensing residues in the s2 and s4 segments of the shaker K+ channel. Neuron. 1996; 16(6):1159–1167. [PubMed: 8663992]

Sigg D, Stefani E, Bezanilla F. Gating current noise produced by elementary transitions in shaker potassium channels. Science. 1994; 264(5158):578–582. [PubMed: 8160016]

Sokolov S, Scheuer T, Catterall WA. Ion permeation through a voltage-sensitive gating pore in brain sodium channels having voltage sensor mutations. Neuron. 2005; 47(2):183–189.10.1016/j.neuron.2005.06.012 [PubMed: 16039561]

Sokolov S, Scheuer T, Catterall WA. Gating pore current in an inherited ion channelopathy. Nature. 2007; 446(7131):76–78.10.1038/nature05598 [PubMed: 17330043]

Sokolov S, Scheuer T, Catterall WA. Ion permeation and block of the gating pore in the voltage sensor of $Na_V1.4$ channels with hypokalemic periodic paralysis mutations. J Gen Physiol. 2010; 136(2):225–236.10.1085/jgp.201010414 [PubMed: 20660662]

Souza CS, Amaral C, Treptow W. Electric fingerprint of voltage sensor domains. Proc Natl Acad Sci USA. 2014; 111:17510–17515.10.1073/pnas.1413971111 [PubMed: 25422443]

Starace DM, Bezanilla F. Histidine scanning mutagenesis of basic residues of the s4 segment of the shaker K^+ channel. J Gen Physiol. 2001; 117(5):469–490. [PubMed: 11331357]

Starace DM, Bezanilla F. A proton pore in a potassium channel voltage sensor reveals a focused electric field. Nature. 2004; 427(6974):548–553.10.1038/nature02270 [PubMed: 14765197]

Starace DM, Stefani E, Bezanilla F. Voltage-dependent proton transport by the voltage sensor of the shaker K^+ channel. Neuron. 1997; 19(6):1319–1327. [PubMed: 9427254]

Stühmer W, Conti F, Suzuki H, Wang XD, Noda M, Yahagi N, Kubo H, Numa S. Structural parts involved in activation and inactivation of the sodium channel. Nature. 1989; 339(6226):597–603.10.1038/339597a0 [PubMed: 2543931]

Takeshita K, Sakata S, Yamashita E, Fujiwara Y, Kawanabe A, Kurokawa T, Okochi Y, Matsuda M, Narita H, Okamura Y, Nakagawa A. X-ray crystal structure of voltage-gated proton channel. Nat Struct Mol Biol. 2014; 21(4):352–357.10.1038/nsmb.2783 [PubMed: 24584463]

Tanabe T, Takeshima H, Mikami A, Flockerzi V, Takahashi H, Kangawa K, Kojima M, Matsuo H, Hirose T, Numa S. Primary structure of the receptor for calcium channel blockers from skeletal muscle. Nature. 1987; 328(6128):313–318.10.1038/328313a0 [PubMed: 3037387]

Tempel BL, Papazian DM, Schwarz TL, Jan YN, Jan LY. Sequence of a probable potassium channel component encoded at Shaker locus of drosophila. Science. 1987; 237(4816):770–775. [PubMed: 2441471]

Tiwari-Woodruff SK, Schulteis CT, Mock AF, Papazian DM. Electrostatic interactions between transmembrane segments mediate folding of Shaker K^+ channel subunits. Biophys J. 1997; 72(4): 1489–1500.10.1016/S0006-3495(97)78797-6 [PubMed: 9083655]

Tiwari-Woodruff SK, Lin MA, Schulteis CT, Papazian DM. Voltage-dependent structural interactions in the Shaker K(+) channel. J Gen Physiol. 2000; 115(2):123–138. [PubMed: 10653892]

Tombola F, Pathak MM, Isacoff EY. Voltage-sensing arginines in a potassium channel permeate and occlude cation-selective pores. Neuron. 2005; 45(3):379–388.10.1016/j.neuron.2004.12.047 [PubMed: 15694325]

Tombola F, Pathak MM, Gorostiza P, Isacoff EY. The twisted ion-permeation pathway of a resting voltage-sensing domain. Nature. 2007; 445(7127):546–549.10.1038/nature05396 [PubMed: 17187057]

Tombola F, Ulbrich MH, Isacoff EY. The voltage-gated proton channel Hv1 has two pores, each controlled by one voltage sensor. Neuron. 2008; 58(4):546–556.10.1016/j.neuron.2008.03.026 [PubMed: 18498736]

Treptow W, Tarek M. Environment of the gating charges in the Kv1.2 shaker potassium channel. Biophys J. 2006; 90(9):L64–L66.10.1529/biophysj.106.080754 [PubMed: 16533847]

Tronin AY, Nordgren CE, Strzalka JW, Kuzmenko I, Worcester DL, Lauter V, Freites JA, Tobias DJ, Blasie JK. Direct evidence of conformational changes associated with voltage gating in a voltage sensor protein by time-resolved X-ray/ neutron interferometry. Langmuir. 2014; 30(16):4784–4796.10.1021/la500560w [PubMed: 24697545]

Vargas E, Bezanilla F, Roux B. In search of a consensus model of the resting state of a voltage-sensing domain. Neuron. 2011; 72(5):713–720.10.1016/j.neuron.2011.09.024 [PubMed: 22153369]

Vargas E, Yarov-Yarovoy V, Khalili-Araghi F, Catterall WA, Klein ML, Tarek M, Lindahl E, Schulten K, Perozo E, Bezanilla F, Roux B. An emerging consensus on voltage-dependent gating from computational modeling and molecular dynamics simulations. J Gen Physiol. 2012; 140(6): 587–594.10.1085/jgp.201210873 [PubMed: 23183694]

Villalba-Galea CA. Voltage-controlled enzymes: The new Janus biforms. Front Pharmacol. 2012; 3:161.10.3389/fphar.2012.00161 [PubMed: 22993507]

Wang MH, Yusaf SP, Elliott DJ, Wray D, Sivaprasadarao A. Effect of cysteine substitutions on the topology of the S4 segment of the Shaker potassium channel: implications for molecular models of gating. J Physiol. 1999; 521(Pt 2):315–326. [PubMed: 10581304]

Xu Y, Ramu Y, Shin HG, Yamakaze J, Lu Z. Energetic role of the paddle motif in voltage gating of Shaker K(+) channels. Nat Struct Mol Biol. 2013; 20(5):574–581.10.1038/nsmb.2535 [PubMed: 23542156]

Yang N, Horn R. Evidence for voltage-dependent S4 movement in sodium channels. Neuron. 1995; 15(1):213–218. [PubMed: 7619524]

Yang N, George AL Jr, Horn R. Molecular basis of charge movement in voltage-gated sodium channels. Neuron. 1996; 16(1):113–122. [PubMed: 8562074]

Yang N, George AL Jr, Horn R. Probing the outer vestibule of a sodium channel voltage sensor. Biophys J. 1997; 73(5):2260–2268.10.1016/S0006-3495(97)78258-4 [PubMed: 9370423]

Yarov-Yarovoy V, DeCaen PG, Westenbroek RE, Pan CY, Scheuer T, Baker D, Catterall WA. Structural basis for gating charge movement in the voltage sensor of a sodium channel. Proc Natl Acad Sci USA. 2012; 109(2):E93–102.10.1073/pnas.1118434109 [PubMed: 22160714]

Yusaf SP, Wray D, Sivaprasadarao A. Measurement of the movement of the S4 segment during the activation of a voltage-gated potassium channel. Pflugers Arch. 1996; 433(1–2):91–97. [PubMed: 9019737]

Zagotta WN, Hoshi T, Aldrich RW. Shaker potassium channel gating. III: Evaluation of kinetic models for activation. J Gen Physiol. 1994; 103(2):321–362. [PubMed: 8189208]

Zhang L, Sato Y, Hessa T, von Heijne G, Lee JK, Kodama I, Sakaguchi M, Uozumi N. Contribution of hydrophobic and electrostatic interactions to the membrane integration of the Shaker K^+ channel voltage sensor domain. Proc Natl Acad Sci USA. 2007; 104(20):8263–8268.10.1073/pnas.0611007104 [PubMed: 17488813]

Zhang X, Ren W, DeCaen P, Yan C, Tao X, Tang L, Wang J, Hasegawa K, Kumasaka T, He J, Wang J, Clapham DE, Yan N. Crystal structure of an orthologue of the NaChBac voltage-gated sodium channel. Nature. 2012; 486(7401):130–134.10.1038/nature11054 [PubMed: 22678295]

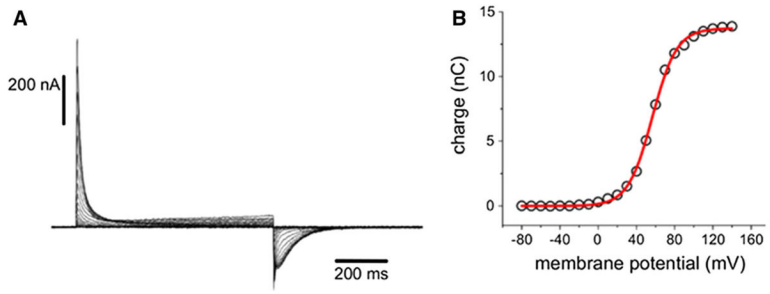

Fig. 1.

Electrical characterization of voltage-sensing motions. **a** Gating (or sensing) currents from the *Ciona intestinalis* voltage-sensing phosphatase C363S mutant expressed in *Xenopus* oocytes. The membrane potential was initially held at −60 mV, and ON sensing currents (upward deflections) were elicited by depolarizing to a potential in the range of −80 to +140 mV using 800-ms test pulses. OFF sensing currents were recorded after repolarization to −60 mV. **b** Corresponding *Q*–*V* curve. Steady-state net charges values calculated by integration of the current traces are plotted against the corresponding membrane potential value. The charge (*Q*) versus membrane potential (*V*) relationship was fitted to a Boltzmann distribution (shown in *red*; see Eq. 1). Adapted from (Villalba-Galea 2012) (Color figure online)

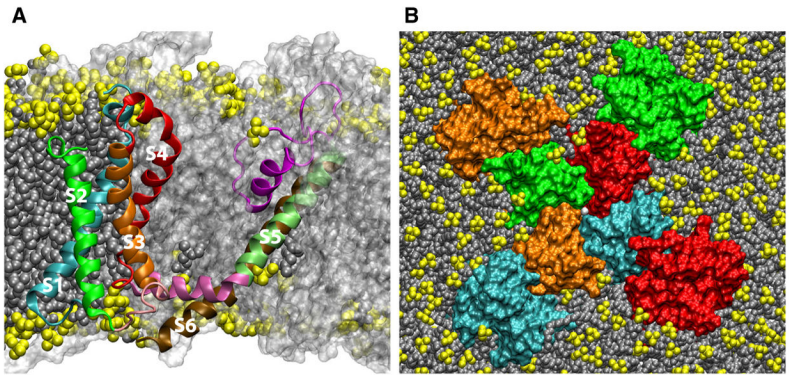

Fig. 2.

The structure of the $K_V1.2$ paddle-chimera channel (Long et al. 2007) in a lipid bilayer. **a** Cut-away view highlighting a single protein chain colored by transmembrane segment (S1, *cyan*; S2, *green*; S3, *orange*; S4, *red*; S5 *lime*; S6, *ochre*). The connecting region between S1 and S2 is not shown for clarity. The other three protein chains are shown in a transparent molecular surface representation colored *white*. Lipids are shown as *filled-spheres* with the headgroups in *yellow*. **b** *Top view*. The pore domain results from the assembly of the S5 through S6 regions of the four protein chains. The four S1–S4 VSDs are on the periphery of the pore domain. The protein chains are shown in a molecular surface representation. Lipids are shown as *filled-spheres* (headgroups in *yellow*) and K^+ ions are shown as *white spheres*. The images correspond to a configuration from an all-atom molecular dynamics simulation of the full-length $K_V1.2$ paddle-chimera channel embedded in a lipid bilayer in excess water (the latter are not shown for clarity) (Color figure online)

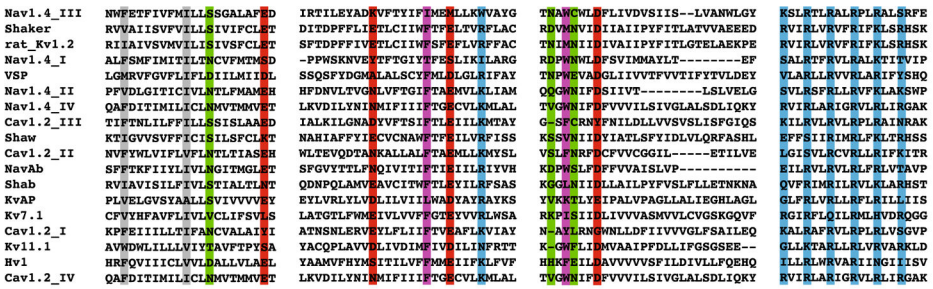

Fig. 3.

Multisequence alignment of S1–S4 VSDs performed by Palovcak et al. (2014). Only the putative transmembrane regions are shown. Sequence positions determined by Palovcak et al. (2014) to be evolutionary “constrained” are shown with a *colored background* according to the most frequent residue type at that position (basic, *blue*; acidic, *red*; polar, *green*; aromatic, *purple*; hydrophobic, *gray* (Color figure online)

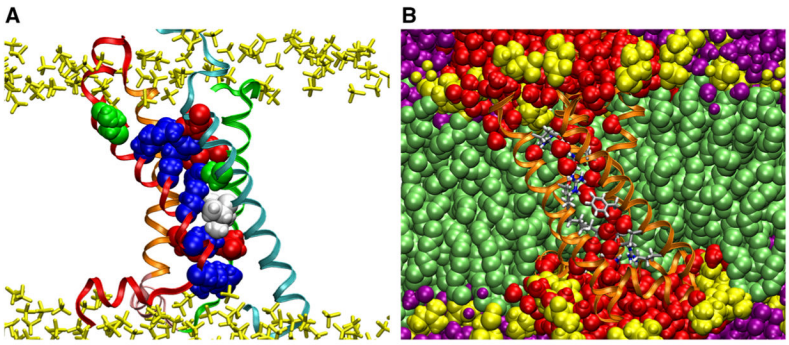

Fig. 4.

VSD structure and solvation. Snapshots from a 12 μs all-atom simulation of the VSD of the $K_V1.2$ paddle-chimera channel (Long et al. 2007) in a lipid bilayer in excess water. **a** The VSD architecture houses two clusters of basic and acidic side chains separated by two hydrophobic residues. The residues determined by Palovcak et al. (2014) to be evolutionary "constrained" are shown as *filled-spheres* (basic, *blue*; acidic, *red*; polar, *green*; hydrophobic, *white*. See Fig. 3 for detailed sequence). The VSD is shown in ribbon representation with the *same color* scheme as in Fig. 2. The lipid phosphate groups are shown in *yellow*. **b** Solvation of the VSD by the membrane. Waters penetrate deeply into the VSD crevices. The VSD is shown in ribbon representation (*orange*) with the conserved residues in licorice representation colored by atom name. Waters within the first two coordination shells of the VSD are shown in *red*. Other waters are in *purple*. Lipids are shown as *filled-spheres* with the headgroups in *yellow* (Color figure online)

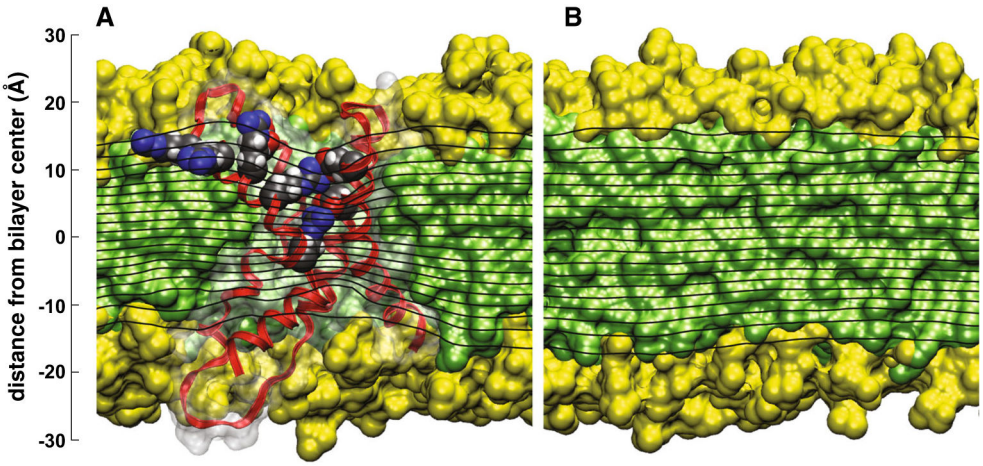

Fig. 5.

VSD electrostatics. **a** The membrane equipotential surfaces (*black lines*; contour interval is 5 % of the applied potential) on a slice passing through the system center of the VSD show focusing features in the crevices that suggest that charges could be displaced across the membrane electric field over a region that is 65.75 % of the membrane thickness. Contributions to the molecular surface from aliphatic chains (*green*), polar groups (*yellow*), and proteins (*white*, transparent) of the corresponding cut-away view are shown as background. The voltage-sensing domain is in ribbon representation (*red*) with the outer four Arg residues in S4, and their salt-bridge partners, shown in *filled-sphere* representation and colored by atom (carbon, *gray*; nitrogen, *blue*; oxygen, *red*; hydrogen, *white*). **b** Similar result for a pure lipid bilayer of the same composition as in **a**. The equipotential surfaces appear parallel to the membrane surface indicating a uniform membrane electric field. The electrostatic potentials were calculated using linearized Poisson–Boltzmann theory, see Krepkiy et al. (2009) and Schow et al. (2010) for details (Color figure online)

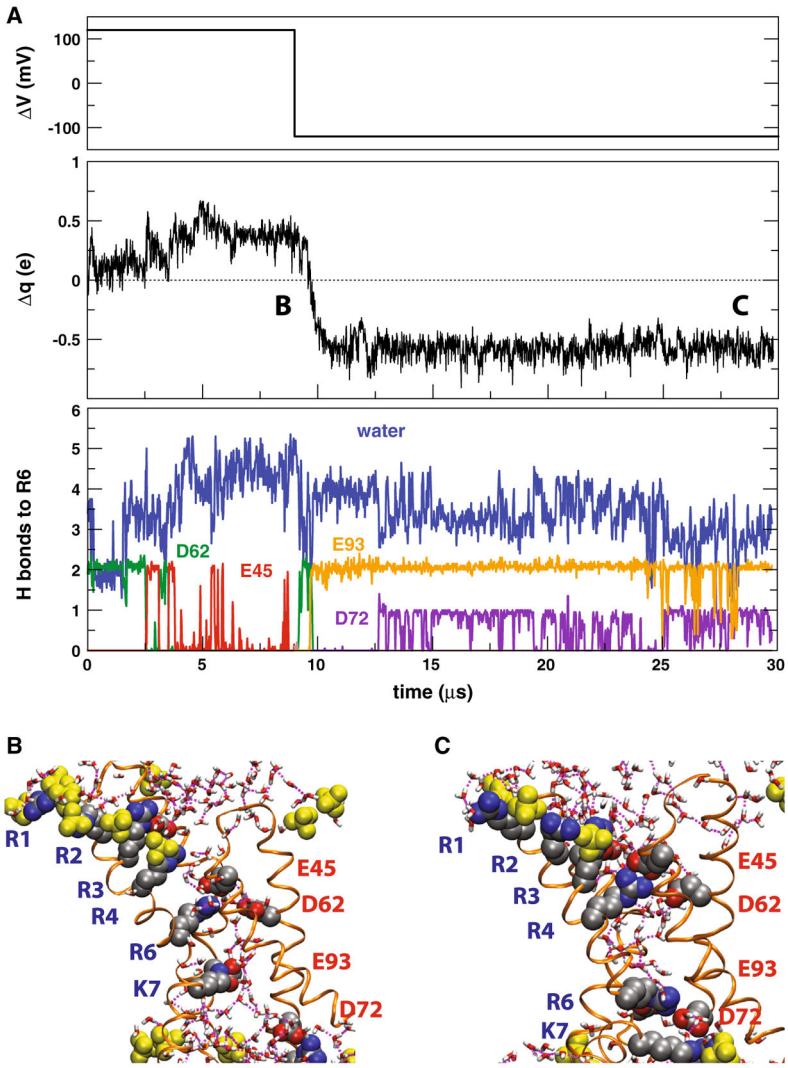

Fig. 6.

Gating charge displacement from an all-atom simulation of the VSD of KvAP in a lipid bilayer under an applied electric field. **a** *(upper panel)* Time dependence of applied membrane potential, Δ*V*, relative to the intracellular side of the membrane. *(middle panel)* Total charge displacement within the membrane electric field with respect to the initial configuration. Switching the membrane potential from a depolarizing to a repolarizing potential after 9 μs produces 1*e* of net gating charge. *(lower panel)* Changes in the solvation environment of R6 as the side chain moves from the center of the VSD into the extracellular cavity (under a depolarizing potential) and from the extracellular cavity to the intracellular cavity (under a repolarizing potential). (**b, c**) Snapshots of the VSD at two membrane potentials: **b** Depolarized ($\Delta V = +120mV$) VSD after 8.5 μs. R4-K7 are shifted outwards with respect to the unpolarized trajectory. **c** Repolarized ($\Delta V = -120mV$) VSD after 28.35 μs. The labels in **a** (*upper panel*) indicate the location of the snapshots within the trajectory. The VSD is shown in secondary structure representation. The conserved charged side chains (shown as *filled-spheres*) are colored by atom type (carbon, *silver*; oxygen, *red*; nitrogen,

blue). The labels (in *blue*) of the basic side chains in S4 follow the order of the triplet repeats starting at the extracellular end (corresponding to R117, R120, R123, R126, R133, and K136 in the KvAP sequence). The conserved positions for acidic side chains are labeled (in *red*) according to the KvAP sequence. Lipid phosphate groups in the first coordination shell of the protein are shown as *filled yellow spheres*. Water molecules in the first coordination shell of the protein are shown in licorice representation colored by atom type (hydrogen, *white*). Water–water hydrogen bonds are drawn as *broken lines*. For clarity, the hydrogen atoms in the protein side chain are not shown. Adapted from Freites et al. (2012) (Color figure online)